Scientific Research Publishing

Open Journal of Geology, 2022, 12, 787-810
https://www.scirp.org/journal/ojg
ISSN Online: 2161-7589
ISSN Print: 2161-7570

The Geological Formations of Koun Fao (East of Côte d'Ivoire): Petrographic Characterization and Associated Deformations

Tokpa Kakeu Lionel-Dimitri Boya*, Fossou Jean-Luc Hervé Kouadio, Allou Gnanzou, Martial Pohn Koffi Adingra, Odrouro Ablan Anne Marie Kouame, Marc Ephrem Allialy

Laboratory of Geology, Mineral and Energy Resources/Training and Research Unit in Earth Sciences and Mineral Resources, Félix Houphouët-Boigny University, Abidjan, Côte d'Ivoire
Email: *lionelboya2000@yahoo.fr

How to cite this paper: Boya, T.K.L.-D., Kouadio, F.J.-L.H., Gnanzou, A., Adingra, M.P.K., Kouame, O.A.A.M. and Allialy, M.E. (2022) The Geological Formations of Koun Fao (East of Côte d'Ivoire): Petrographic Characterization and Associated Deformations. *Open Journal of Geology*, **12**, 787-810.
https://doi.org/10.4236/ojg.2022.1210038

Received: September 6, 2022
Accepted: October 25, 2022
Published: October 28, 2022

Abstract

This study aims to contribute to improve knowledge on geological formations of Comoé basin. The petrographic study of the geological formations of Koun Fao has highlighted two major lithological families: magmatic rocks consisting of monzonites, monzogranites, diorites, biotite granodiorites, syenites, porphyritic micromonzonites and porphyritic dacite and metamorphic rocks from sedimentary origin (quartz schists, meta-greywackes, schists, andalusite chloritoschist and paragneiss). These formations are affected by amphibolite to greenschist facies metamorphism and hydrothermal alteration (pervasive and vein) marked by the presence of quartz, epidotes, chlorites and sericite. Minerals such as andalusite, muscovite and chlorite characterize a local low pressure contact metamorphism in the andalusite chloritoschist. Remote sensing data (Landsat 8 image) coupled with field data allowed the production of a geological map of the area. The study of the structures and microstructures highlighted two deformation mechanisms. These are flattening and simple shear (ductile and brittle). The study area is affected by four deformation phases: D1 marked by a N-S to NNE-SSW elongation, D2 marked by a NW-SE to NNW-SSE compression phase, D3 which is a NE-SW to NNE-SSW transpression phase and D4, responsible for late structures, marked by a NW-SE to NNW-SSE transpression phase.

Keywords

Petro-Structural, Geological Formations, Comoé Basin, Koun Fao, Côte d'Ivoire

1. Introduction

The West African Craton is divided into of two ridges: the Reguibat Ridge in the

north and the Man Léo Ridge in the south. Côte d'Ivoire is located in the southern part of the Man Léo Ridge, which is marked by the Archean and Paleoproterozoic domains in its western and eastern parts, respectively. The Paleoproterozoic domain of Côte d'Ivoire contains most of the Birimian formations of West Africa, which according to some authors are of great interest for mining research [1]. Indeed, Côte d'Ivoire contains a significant portion of birimic terrains with proven mineral potential. But the current national production of gold shows that efforts need to be made. The geology of the country must be studied extensively in order to highlight its geological potential and possible associated mineral resources. In order to understand the geology of Côte d'Ivoire, many geological studies have been carried out on this area [2] [3] [4]. However, the part to which the Comoé basin belongs remains little studied, although it is the object of covetousness of mining companies for its mineral potential. The present study aims to contribute to the improvement of petrographic and structural knowledge of the Comoé basin. It will focus on the petrographic description of the rocks in the study area in order to identify them and it will carry out a structural analysis revealing the associated deformations.

2. Geological Context

Côte d'Ivoire belongs to the Man Léo ridge. This ridge is characterized by two entities separated by the Sassandra transcurrent fault, *i.e.*, the Baoulé-Mossi domain and the Kenema-Man domain. The study area is located in the Baoulé Mossi domain, which occupies the eastern part of the ridge. This domain includes formations of Birimian age [5]. The Kenema-Man domain is located in the western part of the ridge and comprises formations of Archean age. The Archean formations consist of grey banded gneisses of tonalitic composition with intercalations of pink orthopyroxene granulite and charnockites [6] [7]. Intrusives such as calc-alkaline granites are also present.

The study area is located in eastern Côte d'Ivoire, west of the town of Koun Fao. It belongs to the Baoulé-Mossi domain and is located precisely in the northeast of the Comoé basin. The geology of this region is composed of sedimentary and intrusive formations [8]. These formations were emplaced during the Eburnian tectonic-metamorphic event, a major episode of crustal accretion at 2100 Ma [9] [10] [11]. They are characterized by greenschist facies metamorphism.

The study area is composed of metaarenites dominant on metasiltites, metasiltites dominant on metaarenites, quartzites, microconglomeratic metaarenites, mudstones and fluvial sands, diorites and biotite granites (**Figure 1**). According to some previous work [8], the intrusive formations in the study area are affected by dextral and sinistral faults generally oriented NE-SW. As for the metasediments, they are affected by a N-S oriented schistosity marked by the orientation of phyllite minerals.

3. Methodology

The methods used in this study consisted of remote sensing for lineament tracing,

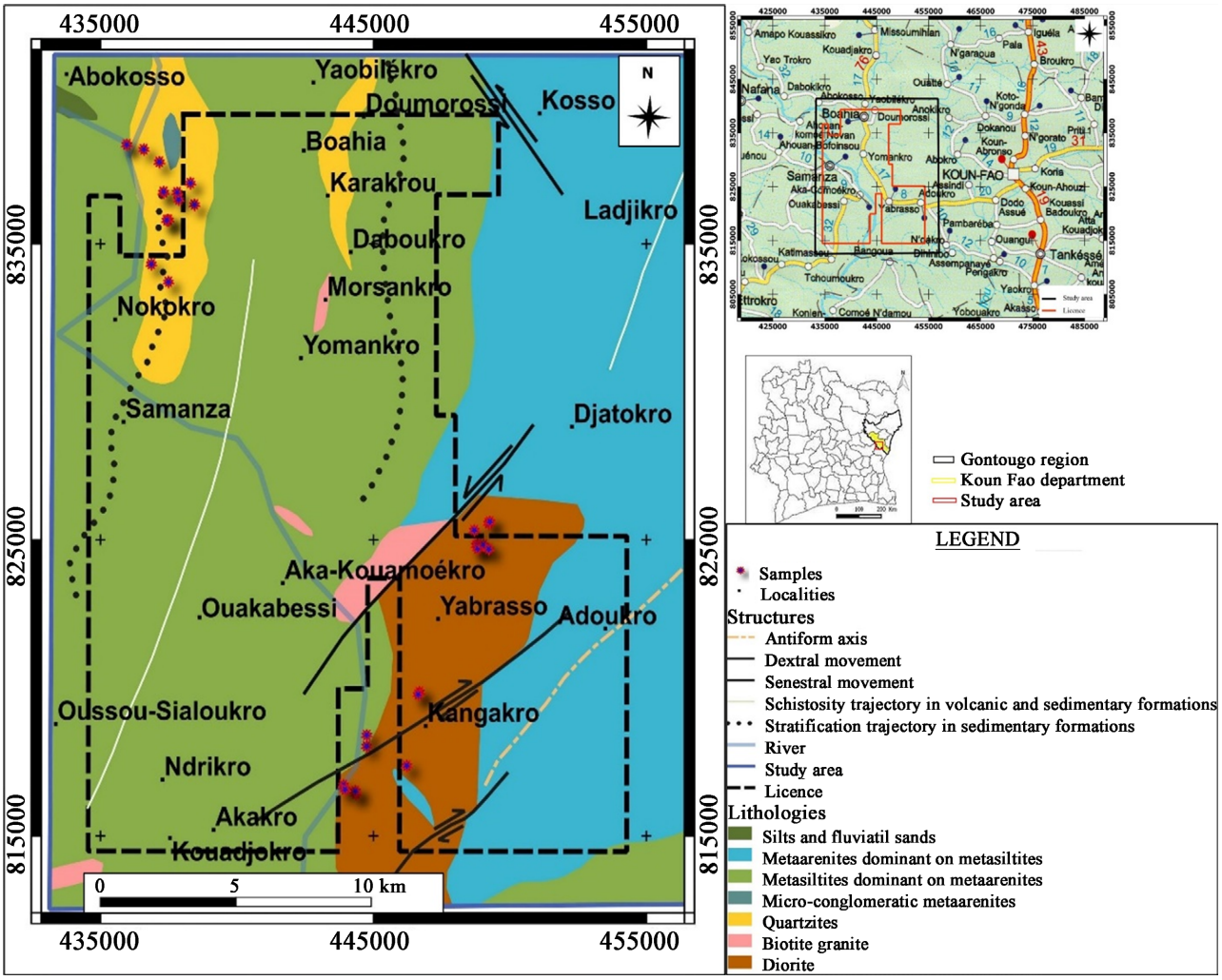

Figure 1. Geological map of the study area showing the different sampling points (Agnibilékro Kouamé-Dari sheet sheet, Siméon *et al.*, 1995, modified).

collection of 28 rock samples in the field and thin section preparation for petrographic description and structural analysis.

3.1. Tele-Analytical Data

Remote sensing techniques use satellite images to improve the location of geological structures and to facilitate the production of refined and accurate lineament mapping [12]. Thus, the remote sensing work on the study area required the use of Landsat 8 images obtained from the USGS platform (https://earthexplorer.usgs.gov/). Landsat 8 is equipped with a multispectral radiometer (OLI) capable of acquiring images in nine spectral bands ranging from the visible to the mid-infrared and a two-channel multispectral infrared radiometer called TIRS. It presents several advantages; of all the Landsat satellites, Landsat 8 is the most advanced. In addition to being freely available, it offers good resolution and allows lithological discrimination and structural characterization. The images obtained were corrected and processed with ENVI 5.2 soft-

ware.

The preliminary image processing phase consisted of eliminating radiometric noise in the various bands and reducing geometric distortions related to the shooting. The processing of the Landsat 8 scene of the study area consisted of a principal component analysis for lineament identification by directional and spatial filtering. The directional filters were applied to the different spectral bands and neo-channels (principal component and band ratios) to obtain the lineament maps. In this study, filtering at the first principal component (CP1) was applied because it contains most of the usual information of the earth from Spots, Landsat, etc. The different filters applied to this first principal component are the YESOU, PREWITT and 00˚, 45˚, 90˚, and 135˚ directional filters which improve the perception of lineaments, corresponding to structural discontinuities, by causing an optical drop shadow effect on the image [13]. Several images were obtained after processing with the directional filters and used to trace the lineaments. However, the one that shows the most image discontinuities is CP1 processed by the YESOU filter (**Figure 2**). The set of lineaments obtained is

Figure 2. Yesou filter applied to the first main composition CP1.

Table 1. Location and coordinates of the samples collected.

Number	Localities	Samples	Easting (WGS 84 zone 30N)	Northing (WGS 84 zone 30N)	Name of the rock
1	Kangakro	AFF1	819,856	446,689	Monzogranite
2	Kangakro	AFF2	819,771	446,643	Monzogranite
3	Nekokro	AFF3	834,313	436,863	Quartz schist
4	Nekokro	AFF4	833,711	437,489	Quartz schist
5	Nekokro	AFF5	838,352	435,968	Schist
6	Nekokro	AFF5b	838,346	435,963	Schist
7	Nekokro	AFF6	838,187	436,587	Meta-greywacke
8	Anoumaba	AFF7	837,764	437,156	Quartz schist
9	Anoumaba	AFF9	835,446	437,489	Quartz schist
10	Anoumaba	AFF12	836,733	437,308	Paragneiss
11	Anoumaba	AFF12b	836,753	437,314	Paragneiss
12	Anoumaba	AFF13	836,321	438,447	Paragneiss
13	Kouakoukrakro-Nekokro road	AFF14	836,735	437,811	Quartz schist
14	Kouakoukrakro-Nekokro road	AO4 et AO4b	836,489	437,866	Meta-greywacke
15	Kouakoukrakro-Nekokro road	AFF15	837,050	438,297	Paragneiss
16	Yabrasso	AFF16	824,847	448,821	Monzonite
17	Yabrasso	AFF16b	448,773	824,811	Diorite
18	Yabrasso	AFF17	448,825	824,700	Diorite
19	Yabrasso	AFF18	449,035	824,827	Monzonite
20	Yabrasso	AFF19	449,228	824,683	Monzonite
21	Yabrasso	AFF20	448,699	825,319	Diorite
22	Yabrasso	AFF21b	449,270	825,609	Micromonzonite
23	Kangakro	AFF22	446,223	817,365	Syenite
24	Kankrakro	AFF23	444,360	816,417	Biotite Granodiorite
25	Kangakro	AFF25	443,907	816,715	Biotite Granodiorite
26	Kangakro	AFF26	444,753	818,023	Biotite Granodiorite
27	Kangakro	AFF28	444,760	818,398	Andalusite Chloritoschist
28	Adoukro	AFF33a	443,715	816,960	Monzonite

imported into the GIS software Qgis 3.10 and Global Mapper 22.1 for the validation phase of the lineament map of the study area. The validation consists of superimposing the lineaments obtained on topographic, road and hydrographic maps and Google Earth images in order to eliminate anthropogenic lineaments [4].

3.2. Macroscopic and Structural Analysis

The macroscopic analysis carried out in the field consisted systematically of a GPS (Global Positioning System) survey of the outcrops (Table 1), their description (mode of outcrop, state of alteration, colour, structure, texture and origin, mineralogy, family) and the relative chronology between outcrops if there were several.

The structural analysis consisted of identifying, describing and recording the structural measurements for each sample when it's possible and establishing the chronology between the different types of deformation observed (schistosities, quartz veins, fractures, vein, etc.). It enabled the different phases of deformation that affected the rocks in the study area to be identified, as well as their characteristics. The structural data was plotted on the Wulf grid using GeOrient software to produce stereographic projections for statistical interpretation of the measurements. Coupled with the field data, the tele-analytical data were used to produce the litho-structural map of the study area. Some of samples collected were oriented before their sending to laboratory.

3.3. Microscopic and Microstructural Analysis

The 28 rock samples led to the preparation of 29 thin sections for microscopic study, *i.e.* a thin section per rock sample, with 2 thin sections from a sample for more details. The study took place at the Geology, Mineral and Energy Resources Laboratory of the Earth Sciences and Mineral Resources Department (UFR STRM) of the University Félix HOUPHOUET-BOIGNY in Abidjan-Cocody. Essentially based on the observation of thin slides with the OPTIKA polarising microscope, it allows a better identification of mineralogical associations and also of microstructures. The mineralogical assemblages and microstructures observed made it possible to refine the petrographic and structural study carried out in the outcrop.

4. Petrographic Characterization

The geological formations in the study area are composed of magmatic rocks and metasediments. The magmatic rocks consist of diorite, monzonite, monzogranite, granodiorite, syenite, microgranodiorite and dacite. The metasediments are composed of schists, andalusite chloritoschist, meta-conglomerate, meta-greywacke and paragneiss.

4.1. Magmatic Rocks

Several different magmatic rocks as mentioned above have been observed in different places of the study area. The lithologies of Yabrasso are composed of monzonite, diorite, porphyry micromonzonite and porphyry dacite while in Kangakro, monzogranite, biotite granodiorite, syenite and diorite have been described. Only monzonite has been observed in Adoukro.

4.1.1. Monzonite

Observed in the localities of Yabrasso and Adoukro, this rock presents itself as a

leucocratic dome, sometimes with numerous quartz veins. Finer-grained mafic enclaves have been found (Figure 3(a)). Microscopically, they have a porphyritic

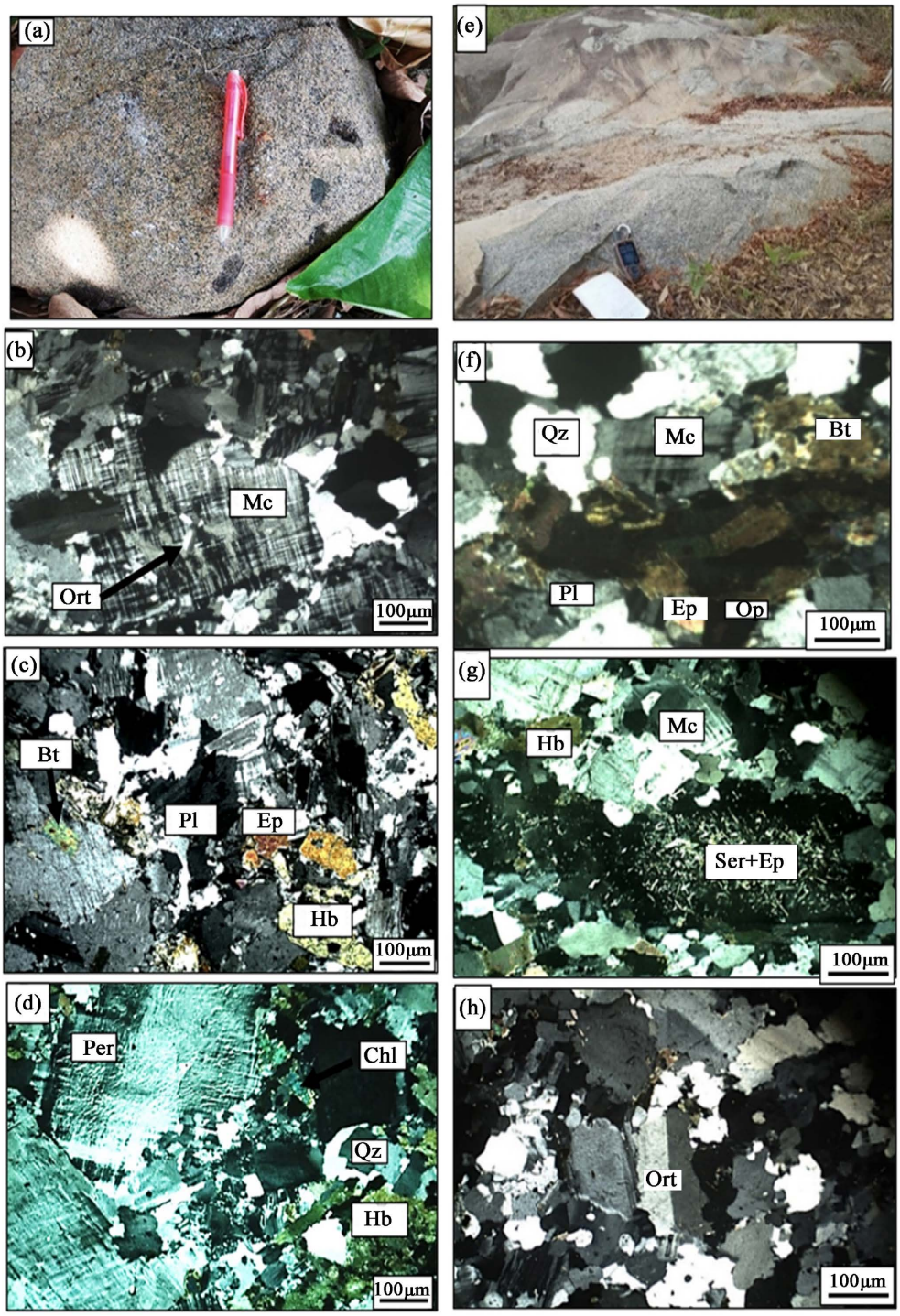

Pl: plagioclase; Mc: microcline; Hb: green hornblende Qz: quartz; Ort: orthose, Per: perthite; Bt: biotite.

Figure 3. Macroscopic and microscopic photographs of monzonites and monzogranites. (a) Monzonite outcrop with mafic enclaves; (b)-(d) mineralogy of monzonites; (e) Monzogranite outcrop; (f)-(h) thin-section monzongranites.

gritty texture with the following mineralogical composition: microcline, plagioclase, perthite, green hornblende, quartz, orthoclase, biotite, chlorite and epidote (**Figures 3(b)-(d)**). About 50-55% of the rock is composed of microcline and plagioclase. These minerals have very particular characteristics. The microclines are surrounded by plagioclase. The perthites are exsolutions that develop in the alkali feldspars. Green hornblende is more abundant than biotite and forms clusters.

4.1.2. Monzogranite

This leucocratic rock outcrops in the form of slabs or domes near the village of Kangakro (**Figure 3(e)**). The outcrops are crossed by numerous quartz veins. Microscopically, it shows a porphyroid gritty texture with the following mineralogical composition: quartz, plagioclase, microcline, orthoclase, biotite, green hornblende, sericite, epidote and sphene (**Figures 3(f)-(h)**). The plagioclase phenocrysts are mostly saussuritised with the formation of sericite and epidote respectively.

4.1.3. Biotite Granodiorite

Observed at Kangakro, these rocks outcrop in elongated form with diorite enclaves (**Figure 4(a)**). Mesocratic and moderately altered, they have a porphyritic gritty texture, with the following mineralogy: quartz, plagioclase, biotite, microcline, green hornblende and sericite (**Figure 4(b)**, **Figure 4(c)**). The quartz is variable in size and subautomorphic to automorphic, with little or no rolling extinction. The plagioclase shows zonations showing that it has been subjected to different physico-chemical conditions than those that allowed its crystallisation. The most dominant ferromagnesian mineral is biotite. Sericite is the only white mica and is mainly found in the heart of the plagioclase from which it was derived.

4.1.4. Syenite

Observed at Kangakro, the syenites outcrop as a dome with a mesocratic colour (**Figure 4(d)**). Microscopically, they have a gritty porphyroid texture and consist of: microcline, perthite, green hornblende, plagioclase, epidote and sphene (**Figure 4(e)**, **Figure 4(f)**). The microcline with a very large size generally contains exsolutions.

4.1.5. Diorite

The diorites outcrop at Yabrasso and Kangakro in elongated, enclave or slab form (**Figure 5(a)**). Mesocratic and moderately altered, these rocks are crossed in places by veins of porphyritic microgranodiorite or by quartz veins. Microscopically, they have a gritty porphyroid texture with a mineralogy composed of: plagioclase, green hornblende, microcline, quartz, biotite, orthoclase, chlorite, epidote and sphene (**Figures 5(b)-(f)**).

4.1.6. Porphyry Micromozonite

Observed at Yabrasso in the form of a dome (**Figure 6(a)**), the texture of this

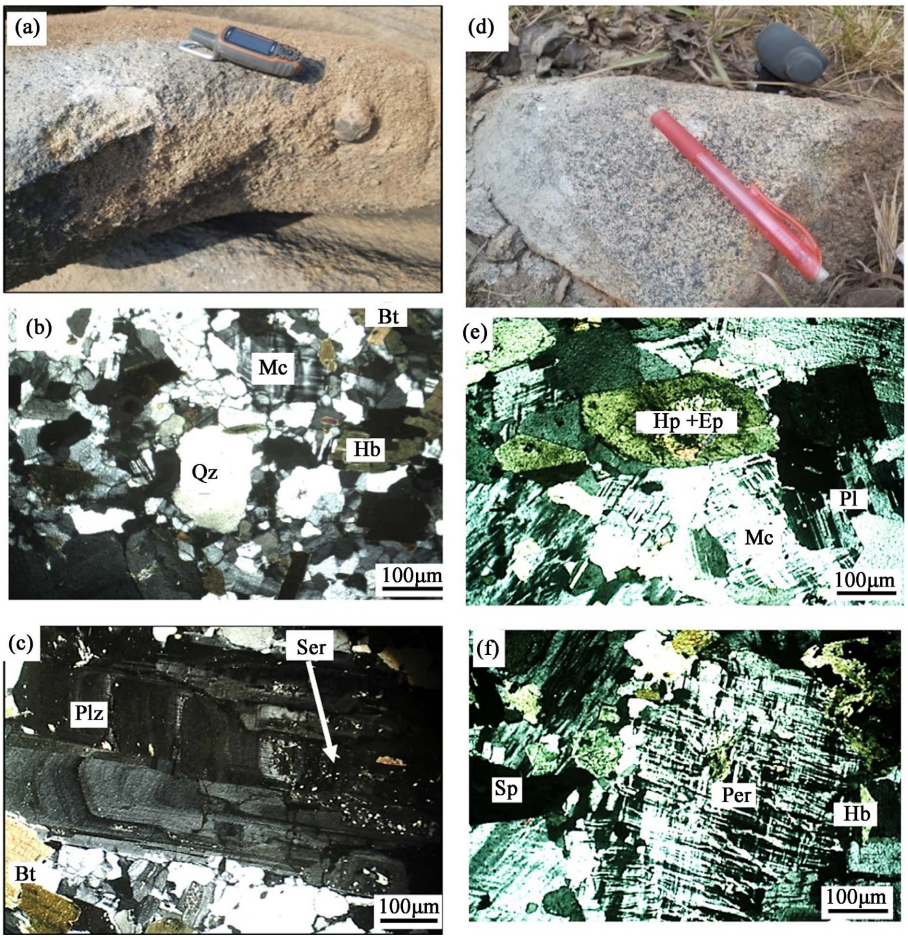

Qz: quartz; Bt: biotite; Mc: microcline; Hb: green hornblende, Plz: zoned plagioclase; Per: Perthite, Ser: sericite, Ep: epidote, Sp: sphene.

Figure 4. Macroscopic and microscopic photographs of biotite granodiorites and syenites. (a) Outcrop of biotite granodiorite; ((b), (c)) mineralogy of biotite granodiorites; (d) outcrop of syenites; ((e), (f)) mineralogy of syenites.

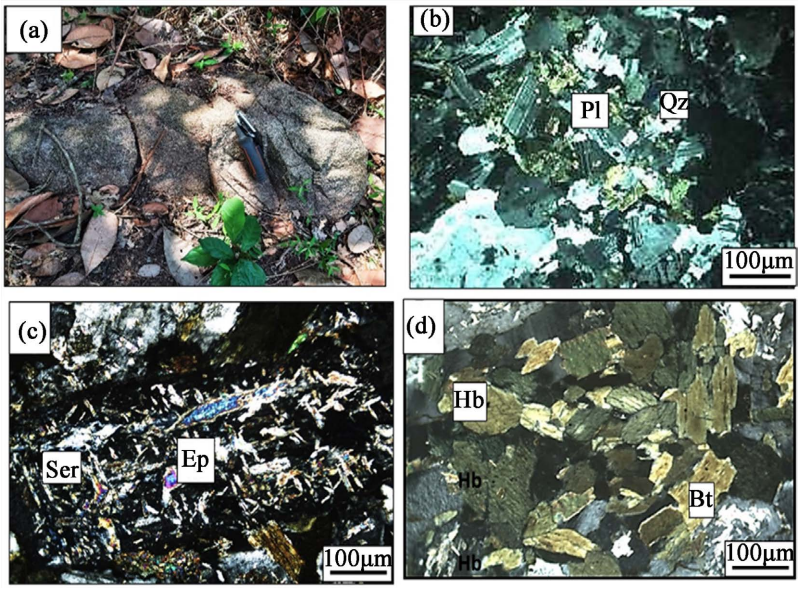

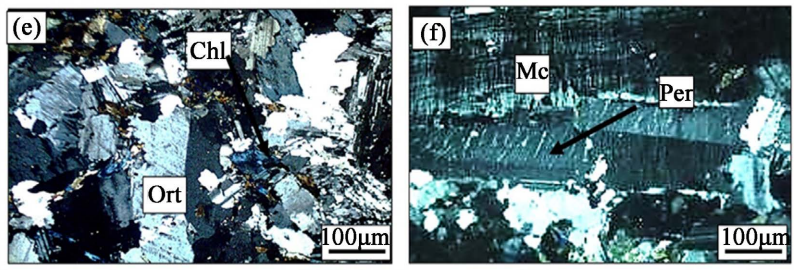

Pl: plagioclase; Mc: microcline; Hb: green hornblende; Chl: Chlorite; Per: Perthite; Ort: Orthose, Ep: Epidote; Qz: quartz; Ser: sericite.

Figure 5. Macroscopic and microscopic photographs of diorites. (a) Diorite outcrop; (b)-(f) Mineralogy of diorites.

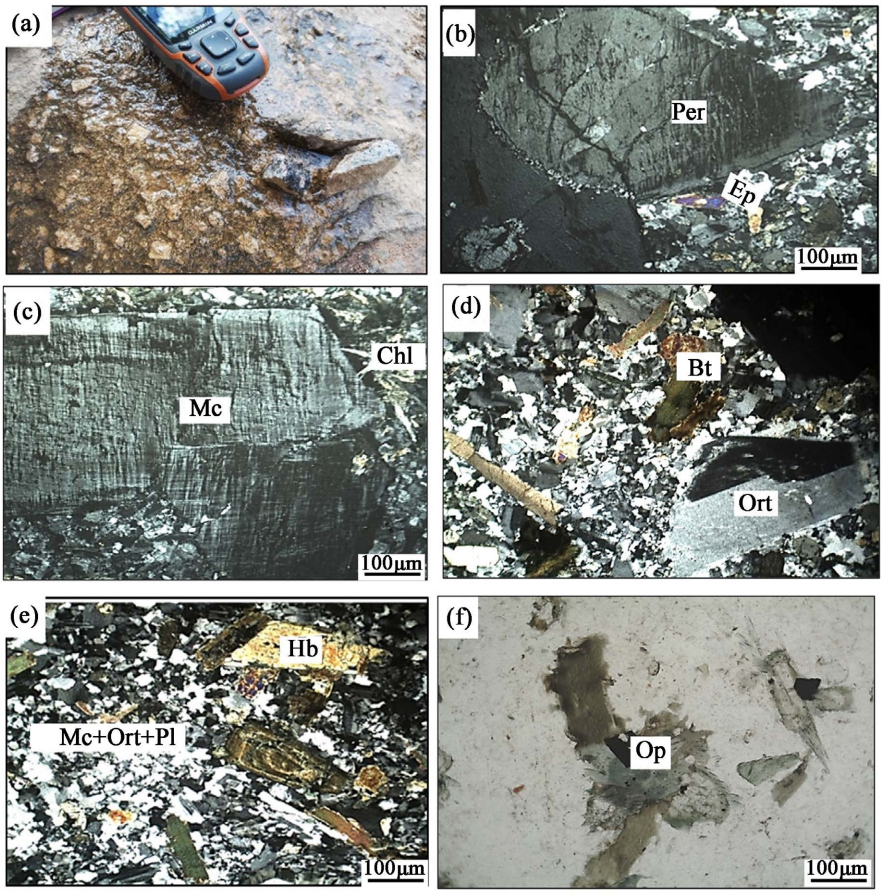

Per: perthite; Bt: biotite; Ep: Epidote; Ort: orthoclase; Mc: microcline; Pl: plagioclase; Hb: green hornblende; Hbz: zoned hornblende; Chl: chlorite; Op: opaque minerals.

Figure 6. Macroscopic and microscopic photographs of porphyry micromonzonites. (a) Porphyry micromonzonite outcrop; (b)-(f) Mineralogy of monzonites.

rock is micrograined porphyry with phenocrysts up to 1 cm in size. Microscopically, it shows a mineralogy composed of: microcline, biotite, orthoclase, plagioclase, hornblende, epidote and chlorite (**Figures 6(b)-(f)**). The microclines are mainly large, sometimes extending beyond the field of view of the microscope. The ferromagnesian minerals in the matrix form aggregates around the feldspars

in the rock.

4.1.7. Porphyry Dacite

This mesocratic rock (**Figure 7(a)**) is observed in diorites and monzonites as a vein. Microscopically, it has a micrograined to microlitic porphyry texture with the following mineralogical composition: quartz, plagioclase, microcline, green hornblende, biotite and chorite. The feldspars of this rock form aggregates (**Figures 7(b)-(d)**). The rock texture based on grains size of matrix seems to attest its sub-volcanic origin, near to surface.

4.2. Mineralogical Characteristics of Magmatic Rocks

Minerals such as plagioclases, amphiboles, biotites and microclines have particular characteristics: ferromagnesian minerals (green hornblende and biotite) are arranged in clusters (**Figure 8(a)**). These mineral accumulations are the result of a segregation process either by gravity, convective flows or by compaction and expulsion of trapped residual liquids [14]. The microclines are surrounded by plagioclase (**Figure 8(b)**). In addition, plagioclases and hornblendes are frequently zoned in the rocks (**Figure 8(c)**, **Figure 8(d)**). These zonations, especially in plagioclase, are complex with sometimes a sericitized core and zones riddled with small inclusions. This indicates that they have been subjected to different physico-chemical conditions than those that allowed their growth in a specific magma. The complexity of their zonation indicates that these crystals were transferred to a magma where they were not in equilibrium. The small

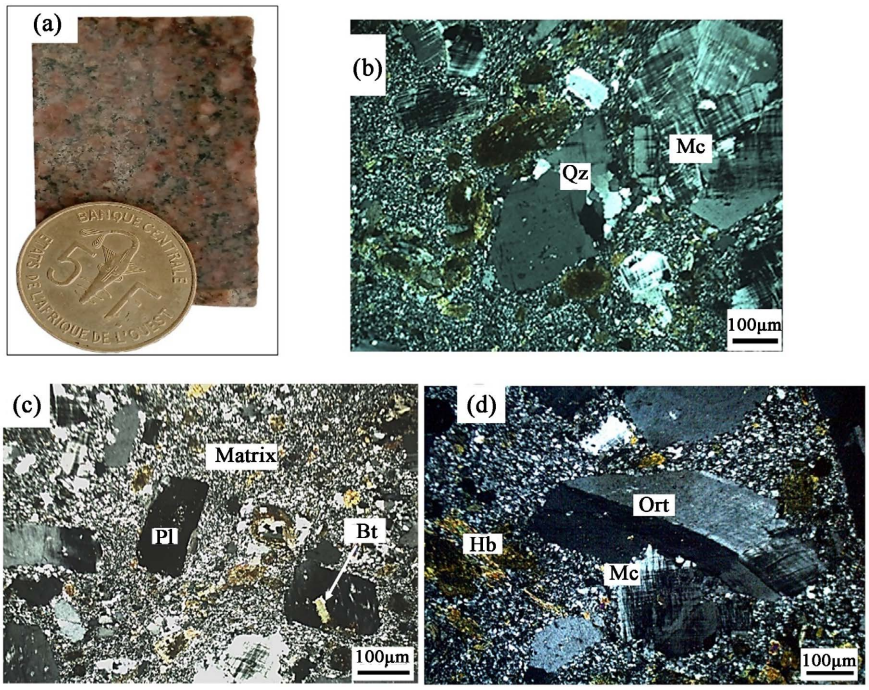

Qz: Quartz; Mc: microcline; Pl: Plagioclase, Hb: Green Hornblende, Per: Perthite; Ort: Orthose, Chl: Chlorite.

Figure 7. Macroscopic and microscopic photographs of the porphyritic dacite.

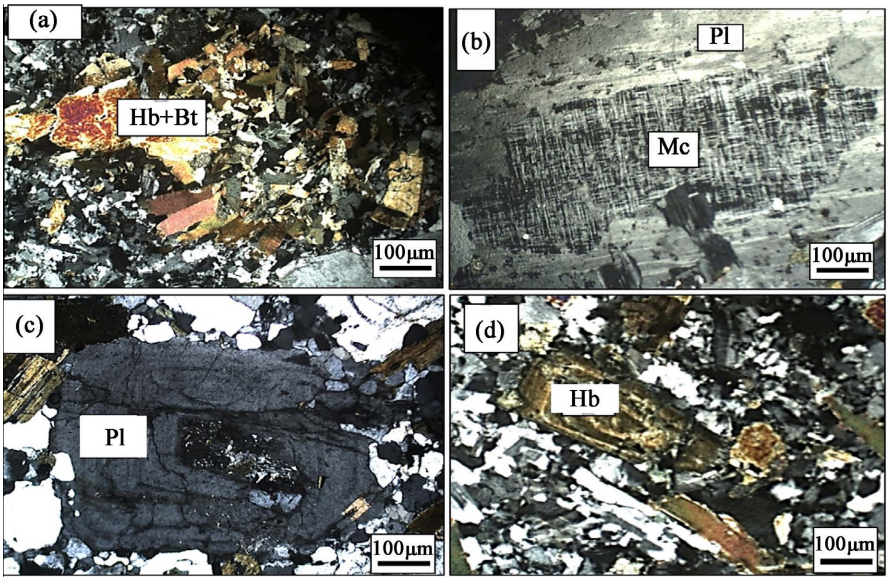

Figure 8. Photomicrographs showing the mineralogy content of magmatic rocks. (a) Cluster of hornblende and biotite; (b) Microcline surrounded by plagioclase; (c) Zoned plagioclase with sericitized core; (d) Zoned hornblende.

inclusions around these crystals mark the fall of the silicate liquid.

4.3. Metamorphic Rocks

4.3.1. Quartz Schist

These are the most dominant metamorphic rocks in the north of the study area, with several outcrops at Anoumaba, Nékokro and along the Nékokro-Kouakoukrakro axis. They are generally affected by a deformation marked by N-S mineral orientation (**Figure 9(a)**). Microscopically, they have a weak granolepidoblastic texture with coarse-grained quartz minerals surrounded by matrix dominated by chlorite, sericite, quartz and muscovite (**Figure 9(b)**, **Figure 9(c)**). These quartz crystals are rounded to subrounded and sometimes angular, with rolling extinction (**Figure 9(c)**). Opaque minerals are also presents (**Figure 9(d)**).

4.3.2. Meta-Greywackes

The meta-greywackes are found in Nékokro and on the Kouakoukrakro-Nékokro axis. These fine-grained rocks are variable in colour (green, grey) (**Figure 9(e)**). Microscopically, they have a granolepidoblastic texture and are composed of quartz, plagioclase, chlorite, orthoclase, muscovite, sericite, epidote and opaque minerals (**Figures 9(f)-(h)**). Chlorite and sericite are secondary minerals resulting from the alteration of biotite, muscovite and plagioclase respectively. Muscovite forms with chlorite and sericite the matrix of the rocks and all mark the schistosity.

4.3.3. Schists

These rocks, observed in the bed of the Comoé River at Nékokro, have a massive appearance, grey in colour, very fine grains and show very pronounce schistosity texture. This schistosity can be vizualised on **Figure 10(a)**, with the sheet flow of

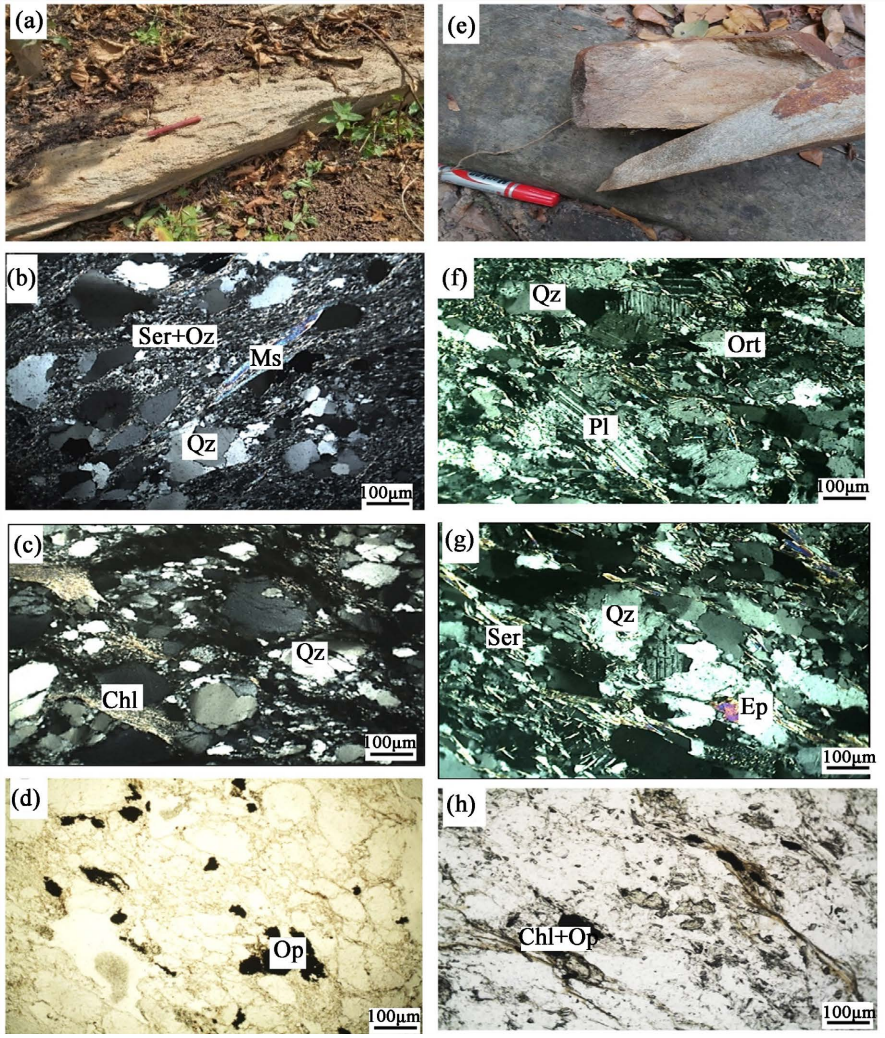

Ser: sericite; Qz: quartz; Chl: chlorite; Ort: orthose; Op: opaque minerals.

Figure 9. Macroscopic and microscopic photomicrographs of quartz schist and metagreywackes.

the rock. Microscopically, these rocks have a lepidoblastic texture, with alternating light bands (quartz) and dark bands (chlorite, sericite, epidote) (**Figure 10(b)**). Composed mostly of chlorite, sericite, epidote and quartz, opaque minerals are also present. These minerals are stretched and oriented along the schistosity.

4.3.4. Andalusite Chloritoschist

This rock was observed in the south-eastern part of the study area, more precisely at Kangakro near the Comoé river. It is in the form of a grey dome (**Figure 10(c)**) with very fine grains. Microscopically, the rock has a poikiloblastic texture, with andalusite poikiloblasts (0.15 - 0.3 mm) in a lepidoblastic background composed of chlorite (**Figure 10(e)**). These poikiloblasts include chlorites and muscovites (**Figure 10(d)**). These altered andalusite crystals are corroded at the edge by large patches of more or less automorphic quartz.

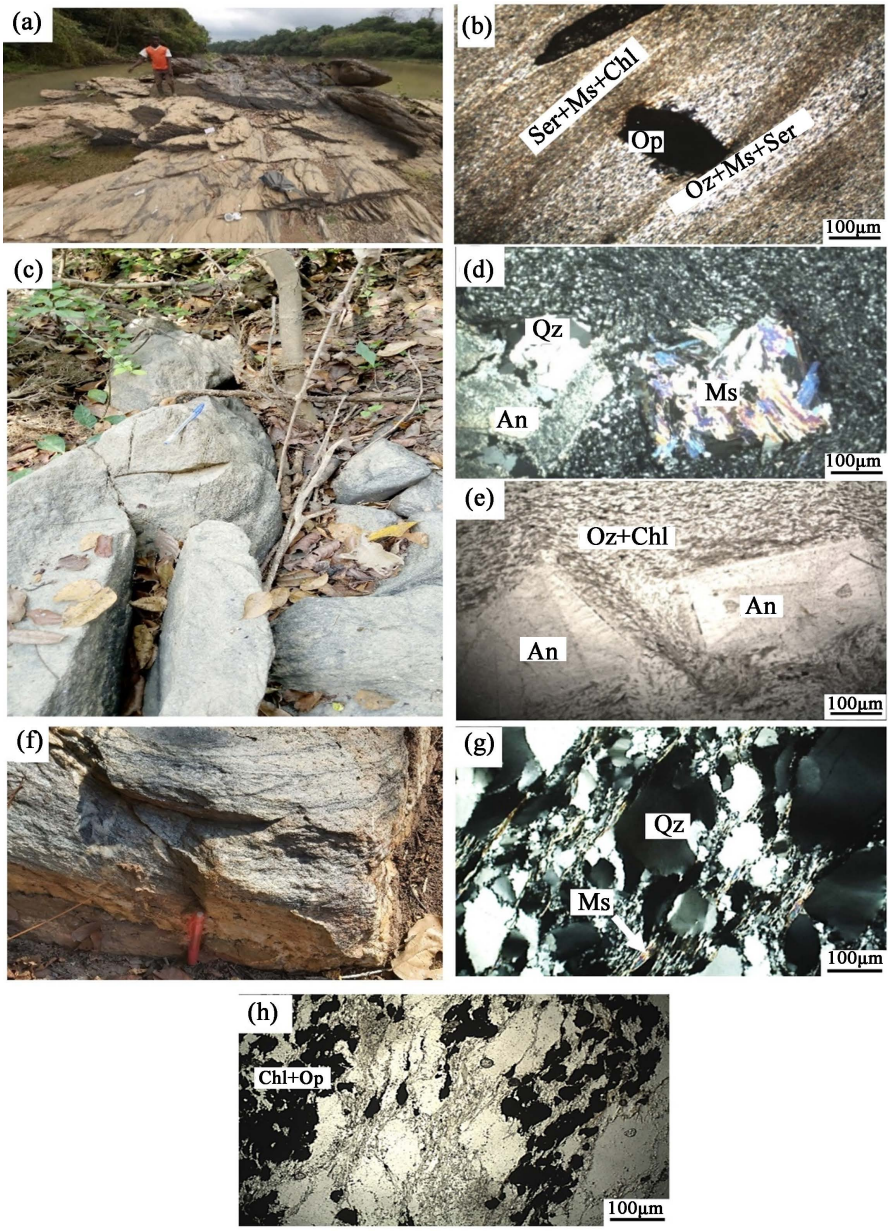

Chl: chlorite, Ser: sericite, Qz: quartz, Ms: muscovite, An: andalusite, Op: opaque minerals.

Figure 10. Macroscopic and microscopic photographs of shale, andalusite chloritoschist and paragneiss.

4.3.5. Paragneiss

Outcrop exposure of paragneiss mostly at Anoumaba (**Figure 10(f)**) and is characterized by alternating light and dark bands foliation. The dark bands are composed of sericite and chlorite, while the light bands are composed of quartz with grain size from 0.1 to 0.3 mm. Microscopically, the rocks have a granolepidoblastic texture and are composed of quartz, muscovite, chlorite and opaque minerals (**Figure 10(g)**, **Figure 10(h)**). The very coarse quartz beds show rolling extinction. The opaque minerals associated with chlorite form ferromagnesian bands marking the foliation.

5. Structural Characterization

The structural data are the result of tele-analytical processing on the one hand and the description of outcrops in the field on the other.

5.1. Tele-Analytical Data Processing

The visual and manual interpretation of the remote sensing images resulted in a lineament map. The analysis of this map led to the identification of different lineament families (Figure 11). Indeed, the map shows 209 data of lineaments whose orientations and lengths vary considerably. These lineaments mostly represent tectonic structures. The directional rosette of the lineaments shows two (2) major directions, the main one being NNW-SSE and the secondary one being ENE-OSW. Lineaments with directions between N156˚ and N180˚ are the most numerous (33.01%), followed by lineaments between N46˚ and N90˚ (26.31%), lineaments between N00˚ and N45˚ (22.49%) and finally lineaments between 91˚ and 155˚ (18.18%). Field evidence within the study area revealed:

- NNW-SSE oriented lineaments are represented by fractures, quartz veins and foliations;
- ENE-WSW oriented lineaments are represented by fractures and quartz veins.

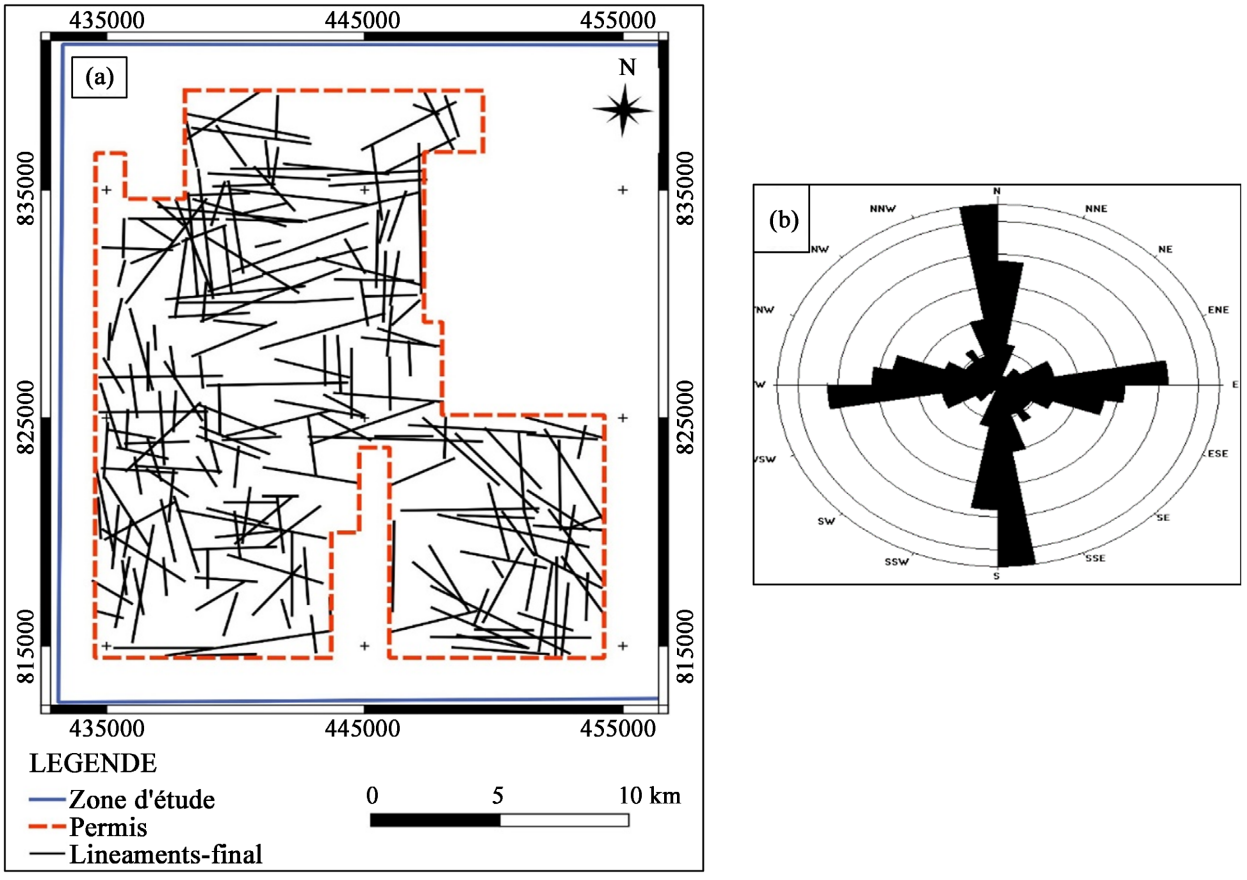

Figure 11. Lineament map and directional rosette of the study area. (a) Lineament map; (b) Directional rosette of lineaments.

5.2. Mesostructures

In the field, the structures observed are schistosity, mineral stretching lineations, foliations, fractures and quartz veins. A detailed analysis of these different structures shows that the study area is affected by four deformation phases. The characteristic structures of these different deformation phases are distinct. Indeed, phase D1 is characterised by ductile structures and phases D2, D3 and D4 are characterised by conjugated brittle structures. The ductile structures are mainly observed in the metasediments, whereas the brittle structures are found in all lithologies.

Deformation phase D1. This first phase is marked by flow schistosity in the metaarenites and metasiltites and by foliation in the paragneisses (**Figures 12(a)-(c)**). These structures are oriented N-S (N0˚-10˚) to NNE-SW (N20˚-25˚) with a general dip towards 20˚E. The schistosity is penetrative in most of the lithologies and is expressed by the preferential orientation of phyllitic and quartz minerals. The use of the directional rosette of these structures indicates a main direction of N-S to NNE-SW (**Figure 12(d)**).

As for the foliation, it is marked by alternating light (marked by quartz minerals) and dark bands which are thought to contain biotite and ferro-titanium oxides (magnetite, hematite, ilmenite) and/or sulphides. The direction of these deformation markers is consistent with an E-W to ONO-ESE oriented shortening.

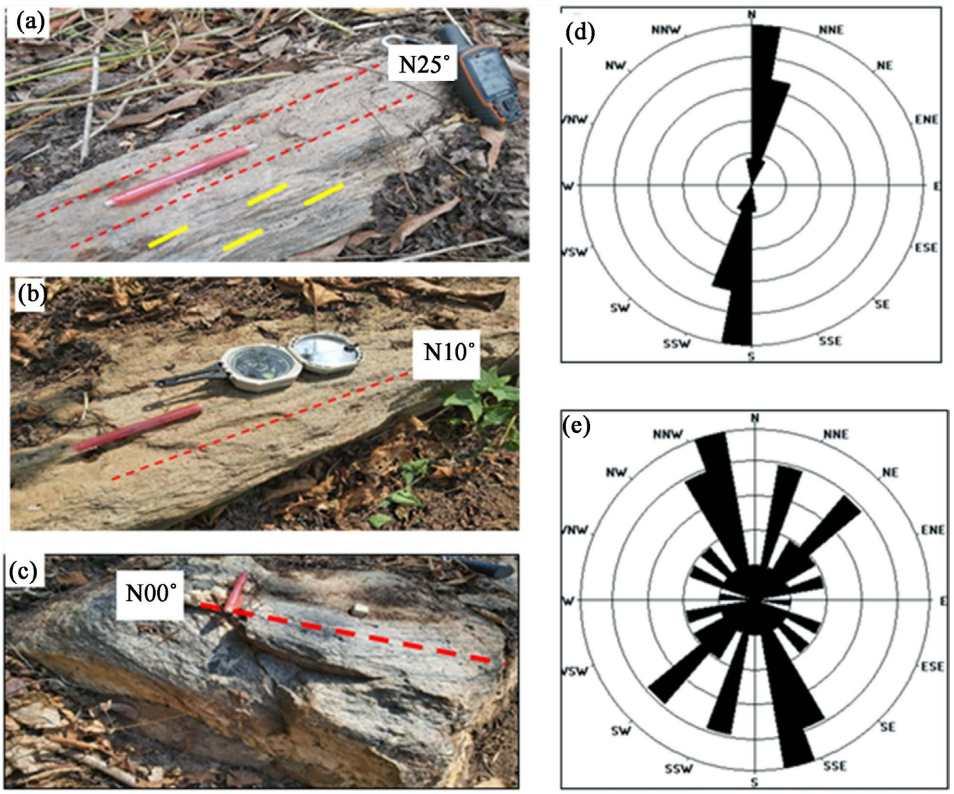

Figure 12. Photographs of ductile structures and directional rosettes of structures in the study area. (a) Schistosity N25˚ and mineral lineation; (b) Schistosity N10˚; (c) Foliation N00; (d) Directional rosette of ductile structures; (e) Directional rosette of brittle structures.

Deformation phase D2. Phase D2 is characterised by quartz fractures and veins (V1) with a direction of N150˚ - N170˚ (Figure 13(a), Figure 13(b)). These brittle structures can be observed in all lithologies of the study area. They intersect the structures of the first deformation D1 and are overtprinted by the structures of D3 and D4 in a sinistral movement.

Deformation phase D3. The D3 phase is marked by quartz fractures and veins (V2 and V3) with a N30˚ - N60˚ direction that overprints the D2 structures in a sinistral movement (Figure 13(a), Figure 13(b)).

Deformation phase D4. The vast majority of the structural data point to a late phase. It is marked by quartz veins and fractures of direction N135˚ - N160˚ (Figures 13(b)-(d)). These structures intersect the structures of D1 and postadate all the other brittle structures in sinistral or dextral movement. In fact, these structures intersecting the previous ones would have been set up by the NW-SE to NNW-SSE transpressive phase.

5.3. Microtextures

Deformation observed on a microscopic scale in magmatic rocks affects plagioclase, feldspar, microcline, orthoclase and quartz. Feldspars, especially plagioclases, contain microfractures filled with quartz and/or feldspars (Figure 14(a), Figure 14(b)). The presence of such microstructure shows that the deformation within these minerals occurred in the presence of magmatic liquid and thus, before the total crystallisation of the magma. This phenomenon is often associated with deformation in granitic rocks [15]. Furthermore, exsolutions of sodium

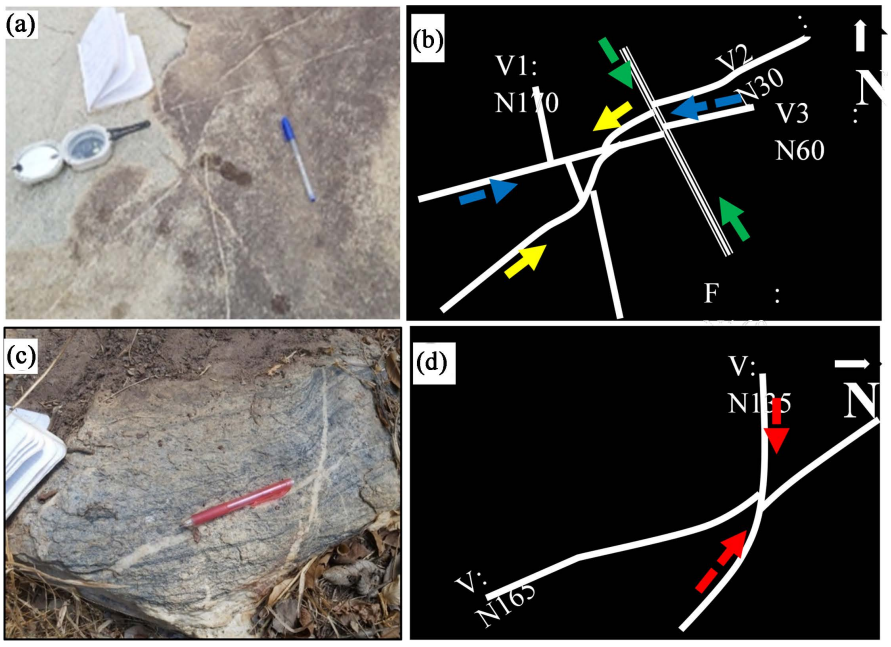

V: Quartz vein; F: Fracture.

Figure 13. Photographs of brittle structures. (a) Veins and fractures observed in a monzogranite; (b) Interpretation of photo a; (c) Quartz veins observed in a paragneiss; (d) Interpretation of photo c.

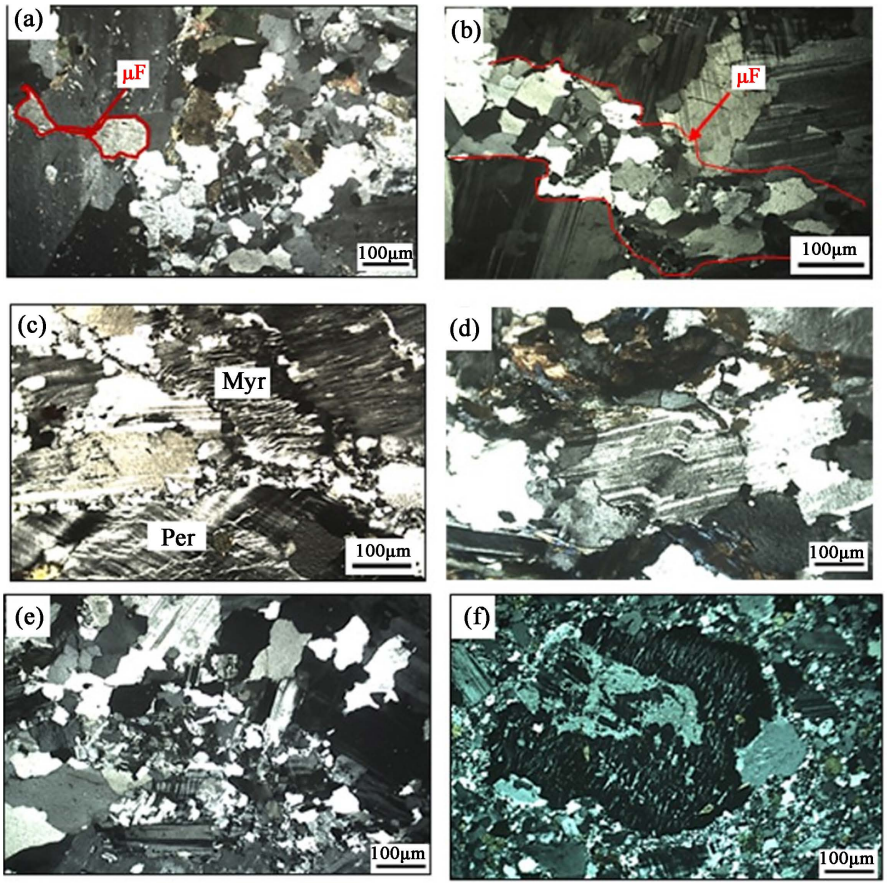

µF: Microfracture; Myr: Myrmekite; Per: Perthite.

Figure 14. Photomicrographs of microstructures in magmatic rocks. ((a), (b)) Microfractures filled with quartz and feldspars and (c) Myrmekite and perthite in monzonite; (d) Micro-kinks in syenite feldspars; (e) Fractured grains at the periphery and recrystallisation with wavy extinction in monzogranite; (f) Dynamic recrystallisation with formation of new grains at the periphery of the large grains in porphyry micromonzonite.

feldspars (perthite) in alkali feldspars develop in monzonite, syenite, diorite; these intergrowths within single crystals results from a process variously called phase separation, unmixing and exsolution, depending on the bulk composition of intergrowth [16]. Myrmekites are also observed at the contact of microcline and plagioclase (**Figure 14(c)**) and their presence corresponds to a phenomenon marking the end of rock consolidation [17]. These microstructures are magmatically to submagmatically dominant. Some deformations are materialised by fractured grains at the periphery of coarse grains with remarkable undulating extinctions, by microkinks, by dynamic recrystallisation with new grain formation at the periphery of old grains (**Figures 14(d)-(f)**).

5.4. Lithostructural Map

The analysis and interpretation of the lineaments (images from the various processing techniques) and the fieldwork have made it possible to produce a lithostructural map of the area (**Figure 15**). The fieldwork highlighted several

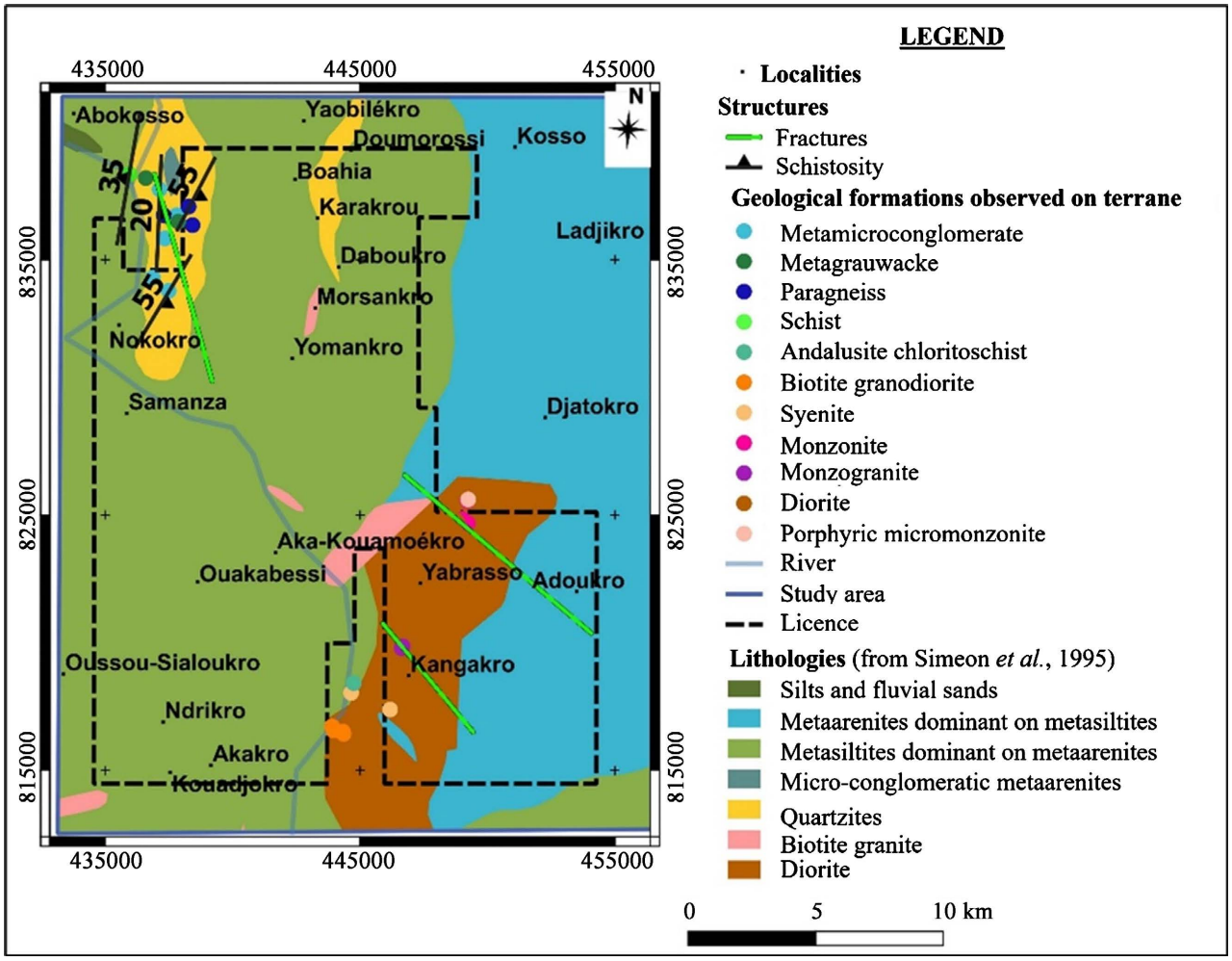

Figure 15. Geological map of the study area (Agnibilékro Kouamé-Dari sheet, Siméon *et al.*, 1995, modified).

geological units in comparison with the existing geological data on the Agnibilékro sheet.

This map summarizes the updated lithologies, schistosities and foliations (in the metasediments) and fractures of the study area. Indeed, this map highlights new geological units such as monzonites, biotite granodiorites, monzogranites, syenites, pophyry microgranodiorites, porphyry micromonzonites, andalusite chloritoschists and paragneisses. In addition to these data, the other information on the map has already been reported by previous authors. Fractures were plotted by associating the coordinates of the points with the lineament boundaries. These fractures affect almost all rocks in the study area and are oriented NW-SE to NNW-SSE. As for the lithological units, the geological contacts could not be exposed due to the cover and alteration. They were therefore represented using the various sampling points by categorization.

6. Discussion

The petrographic study of the geological formations in the study area shows a diversity of rocks: monzonite, monzogranite, biotite granodiorite, diorite, syenite,

porphyritic dacite, porphyritic micromonzonite, quartz schist, meta-greywacke, andalusite chloritoschist and paragneiss. Some of these formations are also observed in other regions of the palaeoproterozoic domain: in the Bondoukou region [18], in Senegal [19], in Ghana [20], in the south-western Comoé basin [21]. The minerals of the magmatic rocks include the clustered arrangement of hornblende and biotites, plagioclases with zonations and microclines that are surrounded by plagioclase. These zonations result from the difference of temperature between core and outer portions and it is linked to changes in metamorphic conditions. The diorites and monzonites are intersected by dacite, which occurs in veins form, and these rocks contain mafic microgranular enclaves. The biotite granodiorite also contains diorite enclaves. According to some authors [14] [22] [23], these mineralogical features and the mafic enclaves are indicative of magma mixing. The presence of mafic microgranular enclaves in monzonites suggests the involvement of a mantle source [24] [25]. According to previous studies [22], the magmatic rocks in the study area seem to be made up of injections of slightly different magmas that were emplaced one after the other, with mantle and crustal origins. The emplacement of these magmas takes place at shallow depth [26], but cooling and crystallisation are relatively long [27]. This could explain the presence of poekilitic potassium feldspar phenocrysts in these rocks. Based on petrographic and mineralogical characteristics, the magmatic rocks of the study area can be considered as hybrid. They are therefore similar to the granitoids studied in the Bondoukou department [28], in the Comoé basin [21] and in central Morocco [29].

The structural analysis shows that the study area is affected by four deformation phases. Phase D1 is a shortening phase oriented E-W to WNW-ESE characterised by N-S to NNE schistosities and foliations. This shortening phase corresponds to the D1 phase described previously [11] as slightly compressive. According to that study, the D1 phase is a N-S to NNE-SW elongation of the massifs, which implies the appearance of initial distensive and then slightly compressive phases in an E-W to WNW-ESE direction. Phases D2, D3 and D4 are characterised by quartz fractures and veins with sinistral components. The direction of these structures reveals that the D2 phase is a NW-SE to NNW-SSE compressional phase, the D3 phase is a NE-SW to NNE-SSW transpressional (compressional-shear) phase and the D4 phase, responsible for the late structures, is a NW-SE to NNW-SSE transpressional phase. These results corroborate those obtained in Ghana [20], in southwest Côte d'Ivoire [30] and in the southwest Comoé Basin [21]. Microstructures such as microfracturing in plagioclase, microkinks, undulating extinctions, dynamic recrystallisation with new grains forming at the edge of old crystals and fractured grains at the periphery of large grains characterise deformation resulting from movement along the dislocation planes [31]. The main mechanisms responsible for this deformation are thought to be brittle fracturing and cataclastic creep; it is therefore a low temperature deformation [32]. Exsolution occurs when, usually as a result of a drop in tem-

perature, a homogeneous phase of a solid solution becomes unstable and separates to form two different minerals. At high temperatures, the crystalline macula vibrates more and creates space to accommodate foreign atoms in the mineral. As the temperature decreases, these atoms are expelled from the macula to form a separate mineral [33]. In the magmatic rocks of the study area, presence of perthite exsolution of sodic feldspars in microcline and orthoclase is evident. As for myrmekite, it marks a simultaneous inter-growth of quartz minerals in a plagioclase solid solution. In monzonites, myrmekitic textures are observed in contact with microcline and plagioclase. They appear to result from the progressive replacement of potassium feldspar by plagioclase [34]. These late-developing structures can be likened to post-magmatic replacements [35] because they succeed the crystallization of the primary minerals of the rock: the inter-growth is slightly late while the progressive replacement is later. Some works [36] interpret microfractures filled with quartzo-feldspar minerals as submagmatic structures. According to these authors, the deformation occurred when the rocks were not yet fully crystallised. Undulating extinctions mark the transition from the submagmatic state to solid state deformation [37].

7. Conclusion

The geological formations in the study area consist of plutonic magmatic rocks with a grainy texture, lode rocks with a micrograiny to microlitic porphyritic texture and metamorphic rocks of sedimentary origin. The magmatic rocks are composed of monzonite, monzogranite, biotite granodiorite, syenite, porphyry micromonzonite and porphyry dacite. The presence of mafic enclaves, mafic mineral clots, normal zonations in plagioclase and microclines surrounded by plagioclase supports the hypothesis of a mixed or hybrid magma at the origin of the formation of plutonic intrusions. Quartz schists, andalusite chloritoschists and meta-greywackes are the metamorphic rocks observed. Microscopic study on all the metamorphic rock shows that the mineralogy is made up of primary minerals (hornblende, biotite, plagioclase, orthoclase, microcline, quartz, opaque minerals) associated with secondary minerals such as chlorite, epidote, sericite. These secondary minerals would come from the alteration of hornblende and biotite (chlorite, epidote), but also from the saussuritisation of plagioclase, microcline, or orthoclase (sericite, epidote) and from the alteration of muscovite (sericite). These paragenesis are common to two levels of metamorphism: high level with markers such as andalousite and a low temperature and pressure environment, that would indicate a retrograde amphibolite to greenschist facies metamorphism. Structural analysis of the various structures (foliations, schistosities, fractures and quartz veins) has identified four phases of deformation in this zone: phases D1, D2, D3 and D4. Phase D1 is characterized by a N-S to NNE-SW oriented S1 schistosity with the presence of remarkable mineral stretching lineations. Phases D2, D3 and D4 are marked by fractures and quartz veins oriented along the main stress direction. They are respectively oriented NW-SE to NNW-SE,

NE-SW to NNE-SW and NW-SE to NNW-SE. The mechanisms responsible for these deformations are flattening and simple shearing. At the microscopic scale, the main deformation mechanisms are brittle fracturing and cataclastic creep.

Acknowledgements

This study was made possible by the management of Stellar Africa Gold based in Vancouver and Geological Research Consulting (GEORECO) based in Abidjan, which we thank for funding and providing optimal conditions.

Conflicts of Interest

The authors declare no conflicts of interest regarding the publication of this paper.

References

[1] Milesi, J.P., Feybesse, J.L., Ledru, P., Dommanget, A., Ouedraogo, M.F., Marcoux, E., Prost, A.E., Vinchon, C., Sylvain, J.P., Johan, V., Tegyey, M., Calvez, J.Y. and Lagny, P. (1989) Les minéralisations aurifères de l'Afrique de l'Ouest. *Chronique de la Recherche Minière*, **497**, 3-98.

[2] Aka, E.B.J.C., Kouamé, L.N., Djroh, S.P., Oboué, Y.A.S.I., Gahé, E. and Sombo, B.C. (2017) Contribution de la géophysique à l'étude de la minéralisation aurifère de Gouméré, Nord-Est de la Côte d'Ivoire: Magnétométrie et polarisation induite. *Afrique SCIENCE*, **13**, 261-272.

[3] Aka, E.B.J.C. (2018) Etude géophysique par magnétométrie et polarisation provoquée des formations précambriennes de la région de Gouméré (Nord-est de la Côte d'Ivoire): Caractérisation lithostructurale et implication à la connaissance de la minéralisation aurifère. Doctorat Université Félix Houphouet-Boigny de Cocody, Cocody, 191 p.

[4] Adingra, M.P.K. (2020) Caractérisation pétro-structurale et géochimie des formations birimiennes de la partie sud-est du bassin de la Comoé Nord d'Alépé sud-est de la Côte d'Ivoire: Implication sur l'évolution géodynamique. Doctorat Université Félix Houphouet-Boigny de Cocody, Cocody, 221 p.

[5] Bessoles, B. (1977) Géologie de l'Afrique: Le craton Ouest Africain. Vol. 1, Bur. Rech. Geol. Min, Mem. 88, 402 p.

[6] Camil, J. (1984) Petrography, Chronology of the Archean Granulitic Ensembles and Associated Formations of the Man Region (Ivory Coast). Implications for the Geological History of the West African Craton. State Thesis, University of Abidjan, Abidjan, 306 p.

[7] Kouamelan, A.N., Peucat, J.J. and Delor, C. (1997) Reliques archéennes (3150 Ma) au sein du magmatisme birimien (2100 Ma) de Côte d'Ivoire, craton ouest-africain. *Comptes Rendus de l'Académie des Sciences*, **324**, 719-727.

[8] Siméon, Y., Delor, C., Zeade, Z., Kone, Y., Yao, B., Vidal, M., Diaby, I., Konan, G., Dje, B.I., N'Da, D., Dommanget, A., Cautru, J.P., Guerrot, C. and Chiron, J.-C. (1995) Notice explicative de la carte géologique de la Côte d'Ivoire à 1/200 000, feuille Agnibilékro. Mémoire de la Direction des Mines et de la Géologie de la Côte d'Ivoire, n˚8, Abidjan, 21 p.

[9] Abouchami, W., Boher, M., Michard, A. and Albarede, F. (1990) A Major 2, 1 Ga Event of Mafic Magmatism in West Africa: An Early Stage of Crustal Accretion.

Journal of Geophysical Research, **95**, 17605-17629.
https://doi.org/10.1029/JB095iB11p17605

[10] Boher, M., Abouchami, W., Michard, A., Albarede, F. and Arndt, N.T. (1992) Crustal Growth in West Africa at 2.l Ga. *Journal of Geophysical Research*, **97**, 345-369. https://doi.org/10.1029/91JB01640

[11] Vidal, M., Delor, C., Pouclet, A., SIméon, Y. and Alric, G. (1996) Evolution géodynamique de l'Afrique de l'Ouest entre 2,2 Ga et 2 Ga; le style "archéen" des ceintures vertes et des ensembles sédimentaires birimiens du nord-est de la Côte d'Ivoire. *Bulletin de la Société Géologique de France*, **167**, 307-319.

[12] Toutin, T. (1996) Opposite Side ERS-1 SAR Stereo Mapping over Rolling Topography. *IEEE Transactions on Geoscience and Remote Sensing*, **34**, 543-549. https://doi.org/10.1109/36.485130

[13] Youan Ta, M., Lasm, T., Jourda, J.P., Kouame, K.F. and Razack, M. (2008) Cartographie des accidents géologiques par imagerie satellitaire landsat-7 etm+ et analyse des réseaux de fractures du socle précambrien de la région de Bondoukou. (Nord-est de la Côte d'Ivoire). *Revue Télédétection*, **8**, 119-135.

[14] Solgadi, F. (2010) Origine et développement de litages dans des roches de composition granitique. Thèse Doctorat, Université du Québec à Chicoutimi, Québec, 458 p. https://doi.org/10.1522/030151515

[15] Simpson, C. and Wintsch, R.P. (1989) Evidence for Deformation-Induced K-Feldspar Replacement by Myrmekite. *Journal of Metamorphic Geology*, **7**, 261-275. https://doi.org/10.1111/j.1525-1314.1989.tb00588.x

[16] Parsons, I. (2021) Feldspars. In: Alderton, D. and Elias, S.A., Eds., *Encyclopedia of Geology*, Second Edition, Academic Press, London, 271-286. https://doi.org/10.1016/B978-0-12-409548-9.12101-3

[17] Dondey, D. (1960) Contribution à l'étude de la série cristallophyllienne et de la couverture sédimentaire de la chaine de Belledonne méridionale (Alpes Françaises). *Travaux de Laboratoire de Géologie, Faculté des Sciences de Grenoble*, **36**, 285-368.

[18] Delor, C., Siméon, Y., Vidal, M., Zeade, Z., Koné, Y., Adou, M., Dibouahi, J., Bi Irié, D., Yao, B.D., N'Da, D., Pouclet, A., Konan, G., Diaby, I., Chiron, J.C., Dommanget, A., Kouamelan, A.N., Peucat, J.J., Cocherie, A. and Cautru, J.P. (1995) Notice explicative de la carte géologique de la Côte d'Ivoire à 1/200,000, feuille de Nassian. Ministère des Mines et de l'Energie, DMG, Abidjan.

[19] Dabo, M. (2011) Tectonique et minéralisations aurifères dans les formations birimiennes de Frandi-Boboti, boutonnière de Kédougou-Kéniéba, Sénégal. Thèse de doctorat des sciences de la terre. Tectonique. Université Rennes l, Rennes, 206 p.

[20] Perrouty, S. (2012) Evolution structurale de la ceinture minéralisée d'Ashanti, SO du Ghana. Thèse, Université de Toulouse, Toulouse, 233 p.

[21] Teha, K.R. (2019) Les formations éburnéennes du sud-ouest du bassin de la Comoé et du secteur de singrobo (sud de la Côte d'Ivoire): Pétrologie, analyse structurale et magmatisme associé. 163 p.

[22] Barbarin, B. (1999) A Review of the Relationships between Granitoid Types, Their Origins and Their Geodynamic Environments. *Lithos*, **46**, 605-626. https://doi.org/10.1016/S0024-4937(98)00085-1

[23] Barbey, P., Gasquet, D., Pin, C. and Ourgeix, A.L. (2008) Igneous Banding, Schlieren and Mafic Enclaves in Calc-Alkaline Granites: The Budduso Pluton (Sardinia). *Lithos*, **104**, 147-163. https://doi.org/10.1016/j.lithos.2007.12.004

[24] Bussy, F. (1990) Pétrogenèse des enclaves microgrenues associées aux granitoïdes

calco-alcalins: Exemple des massifs varisques du Mont blanc (Alpes occidentales) et miocène du Monte Capanne (Île d'Elbe, Italie). Thèse Univ. De Lausanne, Lausanne, 356 p.

[25] Abdallah, N. (2008) Géochimie et géochronologie des intrusions magmatiques panafricaines du terrane Egéré-Aleksod: exemple des massifs granitiques de l'Ounane, Tihoudaine et Tisselliline (Hoggar central, Algérie). Thèse Doc., Univ. Des Sciences et de la Technologie Houari Boumedienne, Algiers, 202 p.

[26] Ague, J.J. (1997) Thermodynamic Calculation of Emplacement Pressures for Batholithic Rocks, California: Implications for the Aluminum-in-Hornblende Barometer. *Geology*, **25**, 563-566. https://doi.org/10.1130/0091-7613(1997)025<0563:TCOEPF>2.3.CO;2

[27] Coleman, D.S., Gray, W. and Glazner, A.F. (2004) Rethinking the Emplacement and Evolution of Zoned Plutons: Geochronologic Evidence for Incremental Assembly of the Tuolumne Intrusive Suite, California. *Geology*, **32**, 433-436. https://doi.org/10.1130/G20220.1

[28] Cassanova, R. (1973) Géochimie et Minéralogie des granitoïdes éburnéens de Côte d'Ivoire. Thèse Doc ès Sc. Univ-Nice, Nice, 327 p.

[29] Haïmeur, J., Chabane, A. and El Amrani, I.E. (2004) Pétrologie et géochimie des granitoides calco-alcalins de Zaër (Maroc central): Modèle pétrogénétique. *Bulletin de l'Institut Scientifique de Rabat, Section Sciences de la Terre*, No. 26, 27-48.

[30] Kouadio, F.J.-L.H. (2017) Etude pétrostructurale des formations géologiques du sud-ouest de la Côte d'Ivoire (secteur blieron-grand bereby): Apport de la géochimie et du couple déformation métamorphisme. Doctorat, Univ. Félix Houphouët-Boigny, Boigny, 221 p.

[31] Stünitz, H., Fitz Gerald, J.D. and Tullis, J. (2003) Dislocation Generation, Slip Systems, and Dynamic Recrystallization in Experimentally Deformed Plagioclase Single Crystals. *Tectonophysics*, **372**, 215-233. https://doi.org/10.1016/S0040-1951(03)00241-5

[32] Passchier, C.W. and Trouw, R.A. (2005) Microtectonics. Springer-Verlag, Berlin, 366 p.

[33] Vernon, R.H. (2004) A Practical Guide to Rock Microstructure. Cambridge University Press, Cambridge. https://doi.org/10.1017/CBO9780511807206

[34] Anouk, L. (2012) Caractérisation structurale et géothermomètre de la suite anorthositique de vallant, Côte-Nord, Québec. Mémoire de la maîtrise en science de la terre. Université du Québec à Montréal, Montréal, 163 p.

[35] Phillips, E.R. (1974) Myrmekite—One Hundred Years Later. *Lithos*, **7**, 181-194. https://doi.org/10.1016/0024-4937(74)90029-2

[36] Bouchez, J.L., Delas, C., Gleizes, G., Nedelec, A. and Cuney, M. (1992) Submagmatic Microfractures in Granites. *Geology*, **20**, 35-38. https://doi.org/10.1130/0091-7613(1992)020<0035:SMIG>2.3.CO;2

[37] Paterson, S.R., Fowler, T.K., Schmidt, K.L., Yoshinobu, A.S., Yuan, E.S. and Miller, R.B. (1998) Interpreting Magmatic Fabric Patterns in Plutons. *Lithos*, **44**, 53-82. https://doi.org/10.1016/S0024-4937(98)00022-X